

---

# MLT-LE: predicting drug–target binding affinity with multi-task residual neural networks

Elizaveta Vinogradova<sup>1,2</sup>, Karina Pats<sup>1,2</sup>, Ferdinand Molnár<sup>2\*</sup>, Siamac Fazli<sup>3\*</sup>,

**1 Department of Biology, Nazarbayev University, Nur-Sultan, Kazakhstan**

**2 Computer Technologies Laboratory, ITMO University, Russia**

**3 Department of Computer Science, Nazarbayev University, Nur-Sultan, Kazakhstan**

\* [ferdinand.molnar@nu.edu.kz](mailto:ferdinand.molnar@nu.edu.kz); [siamac.fazli@nu.edu.kz](mailto:siamac.fazli@nu.edu.kz)

## Abstract

Assessing drug–target affinity is a critical step in the drug discovery and development process, but to obtain such data experimentally is both time consuming and expensive. For this reason, computational methods for predicting binding strength are being widely developed. However, these methods typically use a single-task approach for prediction, thus ignoring the additional information that can be extracted from the data and used to drive the learning process. Thereafter in this work, we present a multi-task approach for binding strength prediction. Our results suggest that these prediction can indeed benefit from a multi-task learning approach, by utilizing added information from related tasks and multi-task induced regularization.

**Availability of implementation:** Associated data, pre-trained models, and source code are publicly available at <https://github.com/VeaLi/MLT-LE>.

## Introduction

One of the early steps in drug discovery is the identification of compounds that have a strong binding to a given target protein. However, due to high costs and time constraints, it is not possible to screen a large subset of the chemical space by performing laboratory experiments. To solve this problem, many computational methods based on machine learning have been developed [1–9]. Most of them are designed to predict one binding constant at a time [1, 3, 5, 6]. However, these methods may struggle to adapt to a new drug–target affinity (DTA) prediction pair due to inconsistency and under-representation of training data [2, 10, 11]. To alleviate this problem, multi-task learning methods have recently been employed [2].

The multi-task approach to molecular property prediction takes advantage of all consistent data by predicting multiple properties simultaneously. By utilizing multiple binding constants at once, multi-task prediction models show improved ability to adapt to new data [2, 7, 10, 12–15]. More technically, multi-task learning is an approach in machine learning that forces a model to favor certain hypotheses over others [12, 16]. Specifically, multi-task learning biases the model toward hypotheses that contribute to the solution of more than one task. Thus, the model’s attention becomes focused on the features that really matter, since multiple tasks provide additional evidence for their relevance or irrelevance, thus ideally providing additional regularization. Therefore, in general,

models trained to solve multiple tasks are more likely to escape the data-dependent noise and find more useful representations [16]. In addition, models trained to solve multiple related tasks simultaneously show less tendency to overfit, generalize better, and have access to more sample data [11, 13, 14, 16, 17].

Multi-task learning can be seen as being inspired by human learning. Humans are able to learn sequentially without forgetting previous knowledge and tend to use the knowledge they already acquired to solve different new tasks [16, 18]. Initially, multi-task learning was introduced to regularize parameters in linear models and evaluate the task relatedness [16]. Nowadays, multi-task learning is used to find solutions to complex problems involving combinations of multiple data sources, such as in bioinformatics [19]. For example, in [19], it was shown that multi-task learning can improve the quality of gene regulatory network reconstruction in settings of scarcely labeled data by using data from multiple organisms simultaneously relying on orthologous genes.

The protein-ligand binding strength can be measured in terms of different binding constants. As a result, there exist several independent datasets. Generally, these datasets are used to train different single-task algorithms. Combining this data would naturally produce more powerful prediction models [12]. However, only a few multi-task drug target binding strength prediction methods have been developed to date [2, 7]. Why is this? Mainly because only few drug target pairs have several measurements available in terms of binding constants. For example, for a dataset with  $\sim 717$  thousand records taken from BindingDB, the complete overlap between the four most common binding constants  $\{K_d, K_i, IC_{50}, EC_{50}\}$  is only 96 records (Fig. 1).

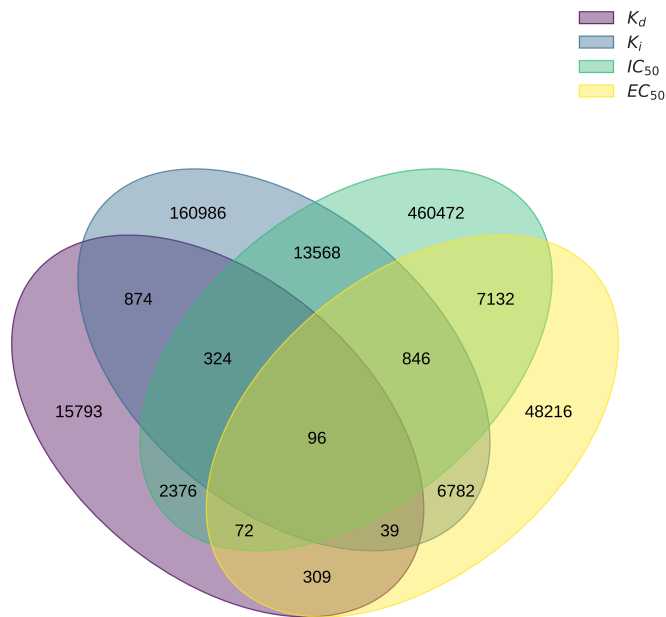


Figure 1. The overlap across all four most commonly expressed binding constants for human drug-target interaction data found in BindingDB is only 96 records (center).

Despite this, a few multi-task methods for drug-protein binding prediction [2, 7] have shown that they are able to exploit multiple overlaps (intersection) of the data and

outperform single-task models in multiple ways [2, 7].

In this work, we propose a new multi-task framework to address the challenges encountered in these related studies [2, 7]. In particular, we propose an approach that allows using all available data (union), including missing values, and using auxiliary tasks to improve performance. We compare our approach with the state-of-the-art GraphDTA framework, which has been shown to outperform most existing methods [5].

## Materials and Methods

### Overview of MLT-LE

We propose a new deep learning framework - MLT-LE for the prediction of binding strength. Existing methods render the binding strength prediction task as a single-task problem, whereas we propose to solve it in a multi-task manner (Fig. 2). The models in our framework are highly adjustable and support multiple drug and target encodings.

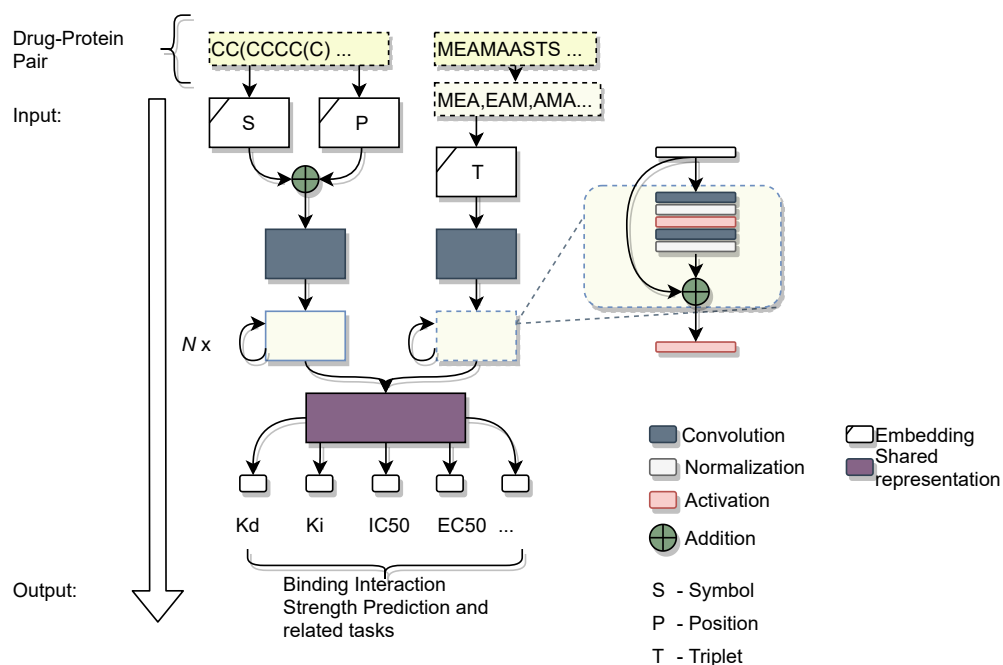


**Figure 2.** General structure of MLT-LE model. The basic structure of the model within MLT-LE is implemented as a residual convolutional network with adjustable depth and number of outputs.

### Handling of missing data

Combining human data from the BindingDB database [20] for any subset of binding constants almost always results in  $> 50\%$  missing data (see table 3 for an example), which makes multi-task approaches challenging to implement. Especially since it has to be solved during algorithm training rather than during the preparation phase, since removing the missing data would greatly reduce the sample size. At the same time, filling in the missing data on such a large scale is impossible. Dahl *et al.* suggested to simply not propagate the error for missing values [17] and Hu *et al.* proposed to use branching - propagating the error only for non-missing values using a separate

---

branch in the neural network [2]. However, usually, when encountering the problem of training an algorithm with missing data points, a technique called masking is used [17]. Masking is the process of dynamically hiding the missing data (i.e. excluding it from the computations) whenever the error is calculated (which is well described for batch optimizers). The error is calculated using some loss function, so masking is part of the loss calculation. In this work, a different loss adjustment is suggested that shows promising results compared to the masking technique. The developed approach proposes to propagate the last non-missing discounted error found, if there is no data available, thus allowing the use of stochastic optimizers.

## Benchmark

To assess the performance of our models, we compare them to the state-of-the-art GraphDTA framework [5]. We used the model hyperparameters for the GraphDTA models (Table 1), as suggested in the original work [5], and compared the performance of all models on the same split of training, validation and test data. Training was conducted for 1000 epochs and the best models were selected based on the performance on the validation data, particularly by monitoring changes in the mean squared error (MSE) for the target variable(s). Subsequently, all the best performing models were used to obtain predictions for unseen sets of test data.

**Table 1.** Models hyperparameters.

Framework	Optimizer	Learning rate	Batch size
GraphDTA	Adam	0.0005	1024
MLT-LE	LookAhead/Nadam with sync. period of 3	0.001	1024

## Complexity

Table 2 gives an overview of the complexity of the models involved in the experiments. As can be seen, the total number of parameters for all models is comparable, although some models solve more tasks. The numbers in the model names indicate the number of layers. The plus sign in the model names indicates that the model is trained on merged  $K_d+EC_{50}$  data (see Section "Data"). The prefix 'Res' indicates that the network has residual connections. For more details on the GraphDTA architecture, please refer to [5].

## Data

In this work, we used human  $K_d$  and  $EC_{50}$  data from BindingDB v2022m3 [20], each divided into 3 sets of the same size, namely train, validation, and test, to mitigate the effects of overfitting. The original subset of human data from BindingDB contained 1,274,797 records, with 525,152 unique SMILES and 1,981 unique amino acid sequences of target proteins. Only records with at least one binding constant were kept. Then, the records were filtered to contain only binding constants recorded without range boundaries, indicated by +- and >< signs. The SMILES sequences were then canonicalized using RDkit-pypi v2022.3.5 [21], and the isomeric information was removed. Only records with valid SMILES strings were kept. As a result, the dataset contained slightly fewer unique SMILES sequences, 498,742. The QED coefficient [22] was then calculated for each SMILES using RDkit (to be used as an auxiliary task later). The individual data records were then aggregated using the median, as was done in [10]. Only valid protein sequences starting with a start codon were considered. Then, the individual records were labeled as "active" or "non-active" drug-target pairs using a threshold of

**Table 2.** Model description.

Framework	Model name	Drug representation	Protein representation	Num. of trainable parameters	Num. of tasks
GraphDTA	GAT2	Graph attention	Convolution	1,460,845	1
	GATGCN2	Graph attention - graph convolution combined		4,749,573	
	GCN3	Graph convolution		2,062,767	
	GIN5	Graph isomorphism		1,297,505	
MLT-LE	ResCNN1	Convolution	Convolution	2,391,783	7
	ResCNN1+				
	ResCNN1GCN4	Graph convolution		2,627,895	
	ResCNN1GCN4+				
	ResCNN1GIN5	Graph isomorphism		2,290,857	
	ResCNN1GIN5+				

$(K_d|K_i|IC_{50}|EC_{50}) < 1\mu M$  for binarization, as done in [23, 24] or similarly in [25]. After that, the training dataset contained a total of 716,342 records. The overlap of records containing different binding constants was then calculated (Fig. 1); the total overlap between records was 96 records in total, with missing values corresponding to more than  $> 77\%$ . Next, only records with  $K_d$  or  $EC_{50}$  non-missing values were kept, yielding 19,796  $K_d$  records and 63,487  $EC_{50}$  records. The data were then shuffled and divided into three equal parts for each set, resulting in 6,598 training, 6,598 validation, and 6,600 test records for  $K_d$  and 21,153, 21,153, 21,155 records for  $EC_{50}$  respectively, all of which contain non-overlapping drug-target pairs. In addition, we created a combined  $K_d+EC_{50}$  dataset, denoted in this work by "+", by combining the training and validation datasets from the separate  $K_d$  and  $EC_{50}$  data. It should be noted that we also saved the target pH information for all datasets in order to use it as another auxiliary task. Table 3 shows the number of non-missing values in the train data for each dataset. Note that the validation and test datasets have a similar distribution of records as the corresponding train dataset.

**Table 3.** Number of non-missing values in train data.

Dataset	$K_d$	$K_i$	$IC_{50}$	$EC_{50}$	active	pH	QED
$K_d$ set	6,598	11	20	1	6,598	580	6,598
$EC_{50}$ set	3	159	201	21,153	21,153	1,144	21,153
Combined ('+')	6,600	170	221	21,153	27,750	1,723	27,750
$K_d + EC_{50}$ set							

## Results

Figure 3 shows the performance of the best models obtained on the test set. It can be seen that the MLT-LE models showed comparable or better performance than the baseline GraphDTA models on all metrics. Additional statistical testing of the observed difference between the predictions of the different frameworks can be found in the supplementary materials. The best scores obtained for each metric are shown in bold.

		RMSE	MSE	$pK_d$			RMSE	MSE	$pEC_{50}$		
				Pearson	Spearman	CI			Pearson	Spearman	CI
GraphDTA	GAT2	1.173	1.376	0.622	0.567	0.705	0.910	0.829	0.792	0.791	0.801
	GATGCN2	1.050	1.102	0.705	0.660	0.745	0.822	0.676	0.805	0.803	0.808
	GCN3	1.090	1.189	0.676	0.625	0.729	0.831	0.690	0.799	0.796	0.805
	GIN5	1.015	1.030	0.729	0.688	0.759	0.805	0.648	0.814	0.812	0.813
MLT-LE	ResCNN1+	1.058	1.119	0.695	0.654	0.740	0.897	0.805	0.776	0.773	0.790
	ResCNN1	1.011	1.022	0.749	0.711	0.769	0.811	0.657	0.822	0.819	0.817
	ResCNN1GCN4+	1.021	1.043	0.730	0.686	0.756	0.815	0.664	0.820	0.817	0.815
	ResCNN1GCN4	<b>0.991</b>	<b>0.983</b>	0.745	0.710	0.769	<b>0.774</b>	<b>0.599</b>	<b>0.834</b>	<b>0.830</b>	<b>0.823</b>
	ResCNN1GIN5+	1.044	1.090	0.723	0.677	0.753	0.819	0.670	0.816	0.814	0.813
	ResCNN1GIN5	0.994	0.988	<b>0.754</b>	<b>0.716</b>	<b>0.771</b>	0.784	0.615	0.829	0.825	0.820

**Figure 3.** Comparison of the model performances on the test set for  $K_d$  and  $EC_{50}$  data. The best scores obtained for each metric are shown in bold.

Figure 4 shows the performance of all models used in the experiment on the validation data. It can be seen that the GraphDTA and MLT-LE framework models show comparable performance, although the GraphDTA models show more stable convergence, while MLT-LE achieves both the highest concordance index ( $CI$ ) and solves more tasks.

It was also observed that the performance of MLT-LE models is also of high quality for other tasks; more information on this is provided in the supplementary material.

In addition, similar model performance was observed when training with a smaller batch size of 256 over 100 epochs for the same datasets (the results of this experiment are shown in the supplementary material).

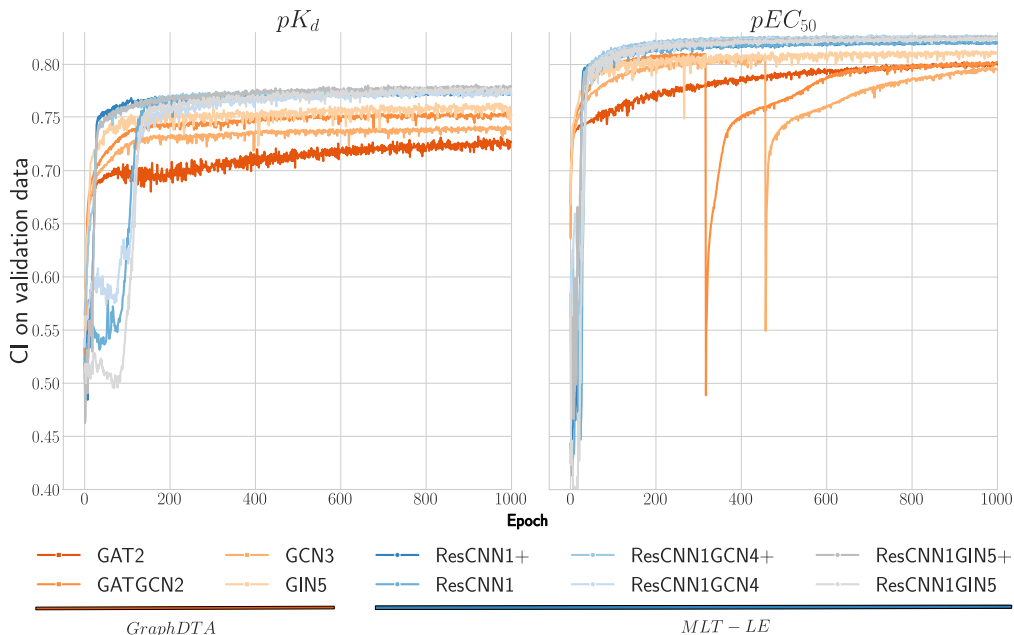


**Figure 4.** Comparison of model performance on the validation data for  $K_d$  and  $EC_{50}$  data. GraphDTA performance is shown in orange and MLT-LE performance is shown in blue.

---

## Discussion

Incorporating data from various sources helps to obtain more accurate predictions of molecular properties [12]. However for this task, the combination of data sources results in a substantial amount of missing data (as can be seen in Table 3). Thus, the question may arise whether combining these data would be beneficial for the prediction [7, 15]. The results of the present work suggest that missing data can be included and is shown to be beneficial in terms of performance (Fig. 3). We attribute this observation to the effect of multi-task models being able to incorporate data from multiple sources and thus utilizing information that is not available for single-task models.

## Conclusion

In this work, we compared our binding strength prediction framework - MLT-LE with the state-of-the-art GraphDTA framework. We tested the performance on two different subsets of BindingDB. We found that MLT-LE performs well for the benchmark datasets across all metrics. We furthermore observed that a multi-task convolutional model can provide comparable results to a single-task graph model, and that a multi-task graph model can perform better than a single-task graph model. We also observed the beneficial effects of incorporating more data, even given the high percentage of missing values.

We believe that it may be possible to further improve performance on the binding strength prediction task using data from more organisms if the orthologous protein sequences in these organisms are matched properly and if a special task is used in the neural network to distinguish the organisms, which can smooth out the effects of different medians of binding constants in these organisms.

## Supporting Information

Associated and supplementary data, data preparation routines, pre-trained models, and source code are publicly available at <https://github.com/VeaLi/MLT-LE>.

## Acknowledgments

The co-authors would like to acknowledge the support of ITMO University Research Grants funding to EV and KP (621314) and Nazarbayev University Research Grants funding to SF and FM (240919FD3926, 091019CRP2108 and 110119FD4520).

## References

1. T. He, M. Heidemeyer, F. Ban, A. Cherkasov, and M. Ester, "SimBoost: a read-across approach for predicting drug–target binding affinities using gradient boosting machines," *J. Cheminformatics*, vol. 9, no. 1, 2017.
2. F. Hu, J. Jiang, D. Wang, M. Zhu, and P. Yin, "Multi-PLI: interpretable multi-task deep learning model for unifying protein–ligand interaction datasets," *J. Cheminformatics*, vol. 13, no. 1, p. 30, 2021.
3. K. Huang, T. Fu, L. M. Glass, M. Zitnik, C. Xiao, and J. Sun, "DeepPurpose: a deep learning library for drug–target interaction prediction," *Bioinformatics*, vol. 36, no. 22-23, pp. 5545–5547, 2020.

- 
4. A. C. A. Nascimento, R. B. C. Prudêncio, and I. G. Costa, “A multiple kernel learning algorithm for drug-target interaction prediction,” *BMC Bioinformatics*, vol. 17, no. 46, 2016.
  5. T. Nguyen, H. Le, T. P. Quinn, T. Nguyen, T. D. Le, and S. Venkatesh, “GraphDTA: predicting drug–target binding affinity with graph neural networks,” *Bioinformatics*, vol. 37, no. 8, pp. 1140–1147, 2021.
  6. H. Öztürk, A. Özgür, and E. Ozkirimli, “DeepDTA: deep drug–target binding affinity prediction,” *Bioinformatics*, vol. 34, no. 17, pp. i821–i829, 2018.
  7. S. Wang, P. Shan, Y. Zhao, and L. Zuo, “GanDTI: A multi-task neural network for drug-target interaction prediction,” *Comput. Biol. Chem.*, vol. 92, no. 9, p. 107476, 2021.
  8. Z. Wu, B. Ramsundar, E. N. Feinberg, J. Gomes, C. Geniesse, A. S. Pappu, K. Leswing, and V. Pande, “MoleculeNet: a benchmark for molecular machine learning,” *Chem. Sci.*, vol. 9, no. 2, pp. 513–530, 2018.
  9. E. Vinogradova, A. Artykbayev, A. Amanatay, M. Karatayev, M. Mametkulov, A. Li, A. Suleimenov, A. Salimzhanov, K. Pats, R. Zhumagambetov, F. Molnár, V. Peshkov, and S. Fazli, “A biologically-inspired evaluation of molecular generative machine learning,” *arXiv*, 2022.
  10. J. Tang, A. Sz wajda, S. Shakyawar, T. Xu, P. Hintsanen, K. Wennerberg, and T. Aittokallio, “Making sense of large-scale kinase inhibitor bioactivity data sets: a comparative and integrative analysis,” *J. Chem. Inf. Model.*, vol. 54, no. 3, pp. 735–743, 2014.
  11. T. Liu, D. Tao, M. Song, and S. J. Maybank, “Algorithm-Dependent Generalization Bounds for Multi-Task Learning,” *IEEE Trans. Pattern Anal. Mach. Intell.*, vol. 39, no. 2, pp. 227–241, 2017.
  12. B. Ramsundar, S. Kearnes, P. Riley, D. Webster, D. Konerding, and V. Pande, “Massively Multitask Networks for Drug Discovery,” *arXiv*, 2015.
  13. Y. Zhang and Q. Yang, “A Survey on Multi-Task Learning,” *arXiv*, 2021.
  14. Y. Zhang, “Multi-Task Learning and Algorithmic Stability,” *Proc. Conf. AAAI. Artif. Intell.*, vol. 29, no. 1, 2015.
  15. Z. Liu, X. Ye, X. Fang, F. Wang, H. Wu, and H. Wang, “Docking-based Virtual Screening with Multi-Task Learning,” *arXiv*, 2021.
  16. S. Ruder, “An Overview of Multi-Task Learning in Deep Neural Networks,” Tech. Rep., 2017.
  17. G. E. Dahl, N. Jaitly, and R. Salakhutdinov, “Multi-task Neural Networks for QSAR Predictions,” Tech. Rep., 2014.
  18. J. Kirkpatrick, R. Pascanu, N. Rabinowitz, J. Veness, G. Desjardins, A. A. Rusu, K. Milan, J. Quan, T. Ramalho, A. Grabska-Barwinska, D. Hassabis, C. Clopath, D. Kumaran, and R. Hadsell, “Overcoming catastrophic forgetting in neural networks,” *Proc. Natl. Acad. Sci.*, vol. 114, no. 13, pp. 3521–3526, 2017.
  19. P. Mignone, G. Pio, S. Džeroski, M. Ceci, G. Pio, S. Džeroski, and M. Ceci, “Multi-task learning for the simultaneous reconstruction of the human and mouse gene regulatory networks,” *Sci. Rep.*, vol. 10, no. 1, p. 22295, 2020.



- 
20. T. Liu, Y. Lin, X. Wen, R. N. Jorissen, and M. K. Gilson, "BindingDB: a web-accessible database of experimentally determined protein-ligand binding affinities," *Nucleic Acid Res.*, vol. 35, pp. D198–D201, 2007.
  21. "Rdkit: Open-source cheminformatics software." [Online]. Available: <https://www.rdkit.org>
  22. G. R. Bickerton, G. V. Paolini, J. Besnard, S. Muresan, and A. L. Hopkins, "Quantifying the chemical beauty of drugs," *Nat. Chem.*, vol. 4, no. 2, pp. 90–98, 2012.
  23. M. Moret, L. Friedrich, F. Grisoni, D. Merk, and G. Schneider, "Generative molecular design in low data regimes," *Nat. Mach. Intell.*, vol. 2, no. 3, pp. 171–180, 2020.
  24. M. Olivecrona, T. Blaschke, O. Engkvist, and H. Chen, "Molecular de-novo design through deep reinforcement learning," *J. Cheminformatics*, vol. 9, no. 1, p. 48, 2017.
  25. F. Grisoni, B. J. H. Huisman, A. L. Button, M. Moret, K. Atz, D. Merk, and G. Schneider, "Combining generative artificial intelligence and on-chip synthesis for de novo drug design," *Sci. Adv.*, vol. 7, no. 24, p. eabg3338, 2021.

# Supplementary Material for “MLT-LE: predicting drug–target binding affinity with multi-task residual neural networks”

Elizaveta Vinogradova<sup>1,2</sup>, Karina Pats<sup>1,2</sup>, Ferdinand Molnár<sup>2\*</sup>, Siamac Fazli<sup>3\*</sup>,

**1 Department of Biology, Nazarbayev University, Nur-Sultan, Kazakhstan**

**2 Computer Technologies Laboratory, ITMO University, Russia**

**3 Department of Computer Science, Nazarbayev University, Nur-Sultan, Kazakhstan**

\* [ferdinand.molnar@nu.edu.kz](mailto:ferdinand.molnar@nu.edu.kz); [siamac.fazli@nu.edu.kz](mailto:siamac.fazli@nu.edu.kz)

Figures 1-2 below show a comparison of model performance on validation and test data when training for 100 epochs with a smaller batch size of 256. This experiment uses the same data partitions and predictive models as the main study. As can be seen in Figures 1-2 the performance of the models can be considered consistent for the two frameworks for two different batch sizes.

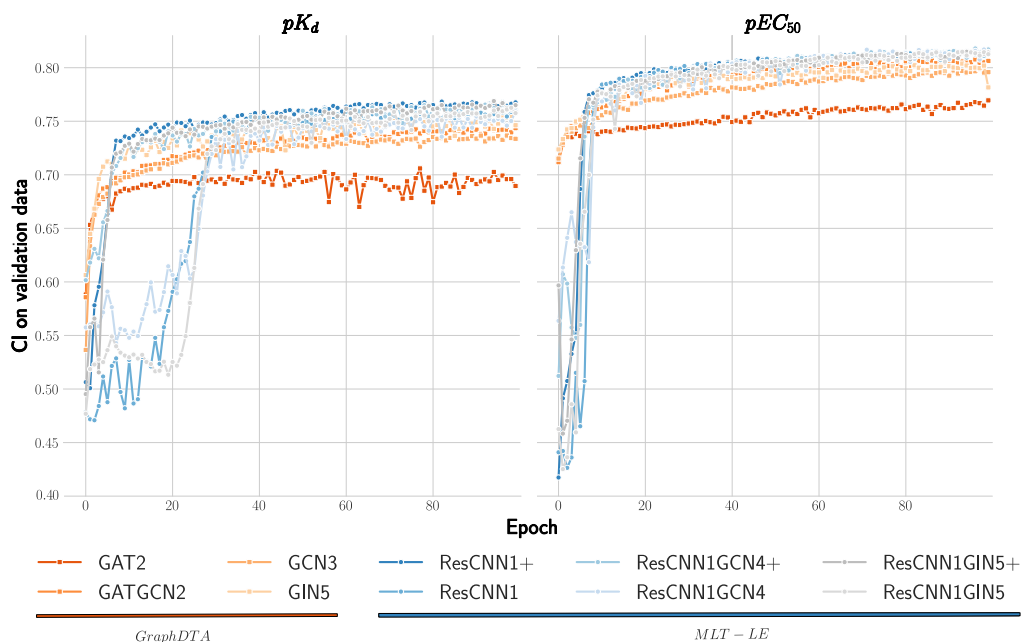


**Figure 1.** Comparison of model performance on the validation data for  $K_d$  and  $EC_{50}$  data when training in 100 epochs with a smaller batch size of 256. GraphDTA performance is shown in orange and MLT-LE performance is shown in blue.

Figure 3 shows the performance of the best MLT-LE model (ResCNN1GCN4) for all tasks  $EC_{50}$  subset test data.

## Statistical significance test of performance on $EC_{50}$ data

It was observed that the prediction accuracy of the GraphDTA models is lower than the prediction accuracy of the MLT-LE models in the test sets. The distribution of

		RMSE	MSE	$pK_d$			RMSE	MSE	$pEC_{50}$		
				Pearson	Spearman	CI			Pearson	Spearman	CI
GraphDTA	GAT2	1.213	1.471	0.576	0.531	0.689	1.034	1.070	0.658	0.644	0.733
	GATGCN2	1.055	1.114	0.703	0.657	0.743	0.823	0.678	0.803	0.802	0.806
	GCN3	1.083	1.172	0.685	0.631	0.733	0.850	0.723	0.791	0.788	0.799
	GIN5	1.065	1.134	0.709	0.667	0.749	0.832	0.692	0.798	0.794	0.802
	ResCNN1+	<b>1.018</b>	<b>1.036</b>	<b>0.735</b>	<b>0.693</b>	<b>0.758</b>	0.850	0.722	0.807	0.804	0.807
MLT - LE	ResCNN1	1.041	1.083	0.729	0.692	<b>0.758</b>	0.831	0.691	0.800	0.798	0.804
	ResCNN1GCN4+	1.036	1.074	0.726	0.687	0.756	0.811	0.658	0.814	0.810	0.811
	ResCNN1GCN4	1.060	1.123	0.716	0.673	0.751	<b>0.794</b>	<b>0.631</b>	<b>0.819</b>	<b>0.815</b>	<b>0.814</b>
	ResCNN1GIN5+	1.028	1.056	0.729	0.688	0.757	0.817	0.667	0.813	0.811	0.811
	ResCNN1GIN5	1.074	1.153	0.722	0.685	0.756	0.809	0.654	0.813	0.810	0.811

**Figure 2.** Comparison of the performances of the best models on the test set for  $K_d$  and  $EC_{50}$  data when training in 100 epochs with a smaller batch size of 256. The best scores obtained for each metric are shown in bold.

predictions between the two best models from each framework for the  $EC_{50}$  dataset can be seen in Fig.4.

In Table 1, we verify that the observed difference in predicted values between the models is statistically significant using a sign test.

**Table 1.** Significance testing

<b>Given:</b>	
N = 21154	Number of predicted values
<b>Two-sided hypothesis:</b>	
$H_0$ : There is no difference between GraphDTA and MLT-LE values	
$H_1$ : There is difference	
<b>Number of positive and negative differences for sign-test:</b>	
11999 - negative differences	Difference between matched pairs of predictions
9155 - positive differences	
<b>Binomial test on pairs of differences:</b>	
Number of trials = 21154	
Number of successes = 11999	
Probability of success = 50%	
P-value: 0.25E-84	
<b>Conclusion</b>	
The null hypothesis can be rejected with a p-value of 0.25E-84.	
The results suggest that the observation of such a difference between pairs of observations or more extreme is unlikely.	

The results of the performed test indicate that the observed difference in performance between the two frameworks in our experiment may be considered significant.

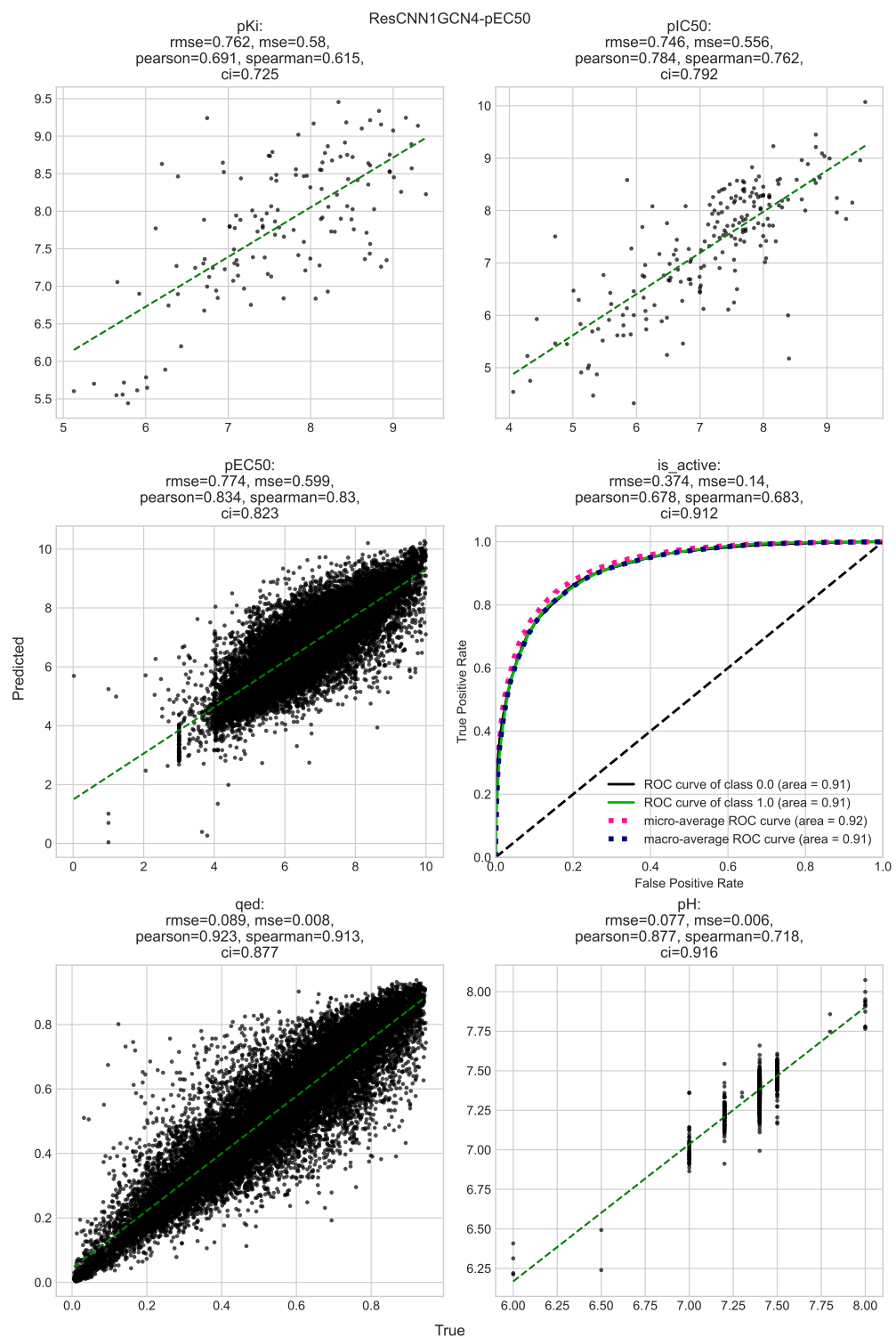


**Figure 3.** Performance of ResCNN1GCN4 model  $EC_{50}$  subset test data

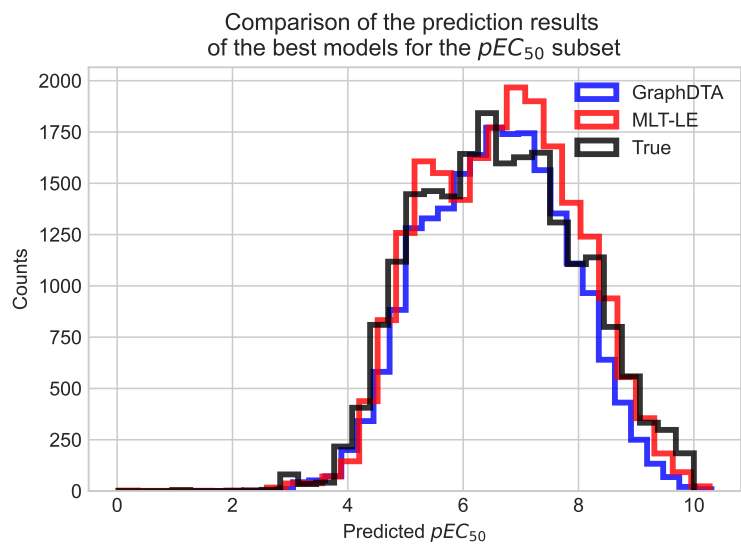


Figure 4. Distribution of predicted values compared to actual distribution